

GRB 060505: A POSSIBLE SHORT-DURATION GAMMA-RAY BURST IN A STAR-FORMING REGION AT A REDSHIFT OF 0.09

E. O. OFEK,¹ S. B. CENKO,¹ A. GAL-YAM,^{1,2} D. B. FOX,³ E. NAKAR,¹ A. RAU,¹ D. A. FRAIL,⁴ S. R. KULKARNI,¹
P. A. PRICE,⁵ B. P. SCHMIDT,⁶ A. M. SODERBERG,¹ B. PETERSON,⁶ E. BERGER,^{2,7,8} K. SHARON,⁹
O. SHEMMER,³ B. E. PENPRASE,¹⁰ R. A. CHEVALIER,¹¹ P. J. BROWN,³ D. N. BURROWS,³ N. GEHRELS,¹²
F. HARRISON,¹ S. T. HOLLAND,¹² V. MANGANO,¹³ P. J. MCCARTHY,⁷ D.-S. MOON,¹ J. A. NOUSEK,³
S. E. PERSSON,⁷ T. PIRAN,¹⁴ AND R. SARI¹

Received 2006 September 11; accepted 2007 March 13

ABSTRACT

On 2006 May 5, a 4 s duration, low-energy, $\sim 10^{49}$ erg, gamma-ray burst (GRB) was observed, spatially associated with a $z = 0.0894$ galaxy. Here we report the discovery of the GRB optical afterglow and observations of its environment using Gemini South, the *Hubble Space Telescope* (*HST*), *Chandra*, *Swift*, and the Very Large Array. The optical afterglow of this GRB is spatially associated with a prominent star-forming region in the Sc-type galaxy 2dFGRS S173Z112. Its proximity to a star-forming region suggests that the progenitor delay time, from birth to explosion, is smaller than ~ 10 Myr. Our *HST* deep imaging rules out the presence of a supernova brighter than an absolute magnitude of about -11 (or -12.6 in the case of maximal extinction) at about 2 weeks after the burst and limits the ejected mass of radioactive ^{56}Ni to be less than about $2 \times 10^{-4} M_{\odot}$ (assuming no extinction). Although it was suggested that GRB 060505 may belong to a new class of long-duration GRBs with no supernova, we argue that the simplest interpretation is that the physical mechanism responsible for this burst is the same as that for short-duration GRBs.

Subject heading: gamma rays: bursts

1. INTRODUCTION

Observations of short gamma-ray burst (GRB) afterglows (e.g., Gehrels et al. 2005; Fox et al. 2005; Hjorth et al. 2005; Berger et al. 2005; Bloom et al. 2006; Nakar 2007) resulted in a possible dichotomy between short GRBs and long GRBs: the presence of a supernova component in long GRBs and its absence from short GRBs. However, the recent discovery of GRB 060614, a 102 s long GRB with no apparent associated supernova (Gal-Yam et al. 2006; Fynbo et al. 2006; Della Valle et al. 2006), may suggest a more complex picture. The situation is further tangled, as the duration distributions of short and long GRBs overlap (e.g., Horváth 2002), and there is no clear way to classify an intermediate-duration GRB on the basis of its duration alone (despite the fashionable 2 s cut). Therefore, intensive multiwavelength observations of nearby GRBs are needed in order to construct a clear picture of the GRB

zoo and to unveil the physical mechanisms behind the different families of GRBs.

On UTC 2006 May 5, at 06:36:01, the *Swift* Burst Alert Telescope (BAT) detected the weak GRB 060505 with a fluence of $(6.2 \pm 1.1) \times 10^{-7}$ erg cm^{-2} in the 15–150 keV band (Palmer et al. 2006; Hullinger et al. 2006) and a T_{90} duration of 4 ± 1 s. The gamma-ray time-averaged spectrum was reported to be well fitted by a simple power law with an index of 1.3 ± 0.3 (i.e., $dN/dE \propto E^{-1.3}$). The on-board detection significance for the burst was below the threshold for an autonomous spacecraft maneuver. Analysis of the full data set on the ground showed the burst to be statistically significant, and a repointing was commanded at ~ 0.6 days. The *Swift* X-Ray Telescope (XRT) detected an X-ray source (Conciatore et al. 2006) at the position R.A.(J2000.0) = $22^{\text{h}}07^{\text{m}}03.2^{\text{s}}$, decl.(J2000.0) = $-27^{\circ}48'57''$. The X-ray position, which has a 90% confidence radius of $4.7''$, is located about $4''$ from the $z = 0.0894$ galaxy 2dFGRS S173Z112 (Colless et al. 2001). Further observations by *Swift* XRT, about 5 days after the GRB, showed that the X-ray source had decayed between the two epochs (Conciatore 2006). In the optical regime, Brown & Palmer (2006) did not detect an optical transient (OT) using *Swift* UltraViolet and Optical Telescope (UVOT) observations of this field conducted ~ 0.6 days after the GRB trigger. However, Ofek et al. (2006) reported the detection of the OT associated with GRB 060505 (see § 2), later confirmed by VLT FORS2 observations (Thöne et al. 2006).

In this paper we present multiwavelength observations of the afterglow and environment of GRB 060505. We present our observations in § 2, derive our basic results in § 3, and discuss their implications in § 4.

2. OBSERVATIONS

Starting 1.09 days after the BAT trigger, we observed GRB 060505 with the Gemini Multi-Object Spectrograph (GMOS) on the Gemini South telescope and obtained imaging data at four

¹ Division of Physics, Mathematics, and Astronomy, California Institute of Technology, Pasadena, CA 91125.

² Hubble Fellow.

³ Department of Astronomy and Astrophysics, Pennsylvania State University, University Park, PA 16802.

⁴ National Radio Astronomy Observatory, Socorro, NM 87801.

⁵ Institute of Astronomy, University of Hawaii, Honolulu, HI 96822-1897.

⁶ Research School of Astronomy and Astrophysics, Mount Stromlo Observatory, Weston, ACT 2611, Australia.

⁷ Observatories of the Carnegie Institution of Washington, Pasadena, CA 91101.

⁸ Princeton University Observatory, Princeton, NJ 08544.

⁹ School of Physics and Astronomy and the Wise Observatory, Tel Aviv University, Tel Aviv 69978, Israel.

¹⁰ Department of Physics and Astronomy, Pomona College, Claremont, CA 91711.

¹¹ Department of Astronomy, University of Virginia, Charlottesville, VA 22903.

¹² NASA Goddard Space Flight Center, Greenbelt, MD 20771.

¹³ INAF, Istituto di Astrofisica Spaziale e Fisica Cosmica di Palermo, I-90146 Palermo, Italy.

¹⁴ Racah Institute of Physics, Hebrew University, Jerusalem 91904, Israel.

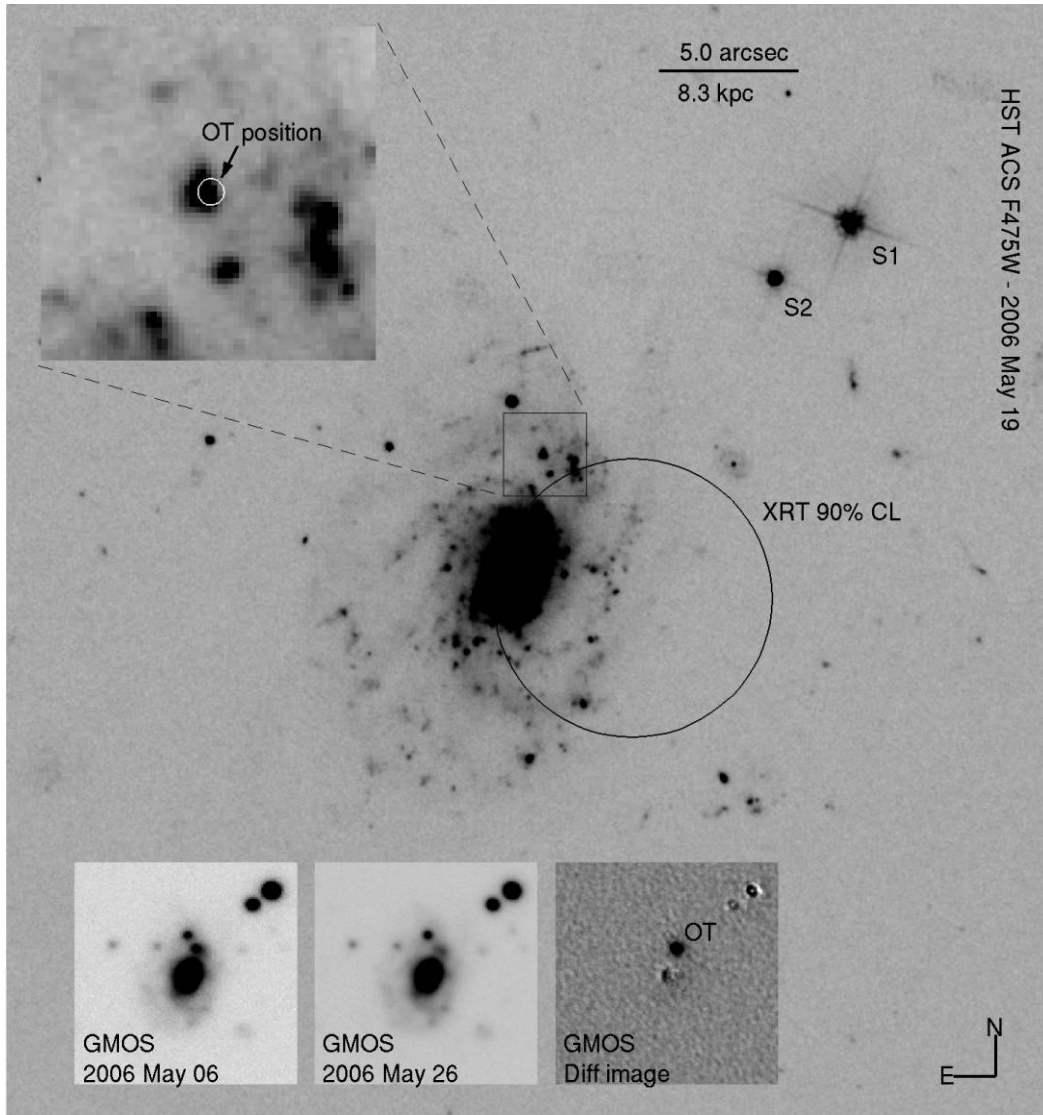


FIG. 1.—First epoch of the *HST* ACS F475W-band image of the GRB host galaxy 2dFGRS S173Z112. The big black circle marks the XRT 90% confidence level (CL) circle. S1 and S2 are the reference stars listed in Table 2. The inset at the upper left corner zooms in on the position of the OT, which is marked by a white circle. The radius of the white circle is $0.12''$, which is the 2σ error on the position of the OT due to the transformation between the GMOS image and the *HST* image. Note that the *Chandra* X-ray position is consistent with the OT position. The insets at the bottom show the *g*-band GMOS first-epoch image (left), the last-epoch image (middle; see Table 1), and the difference image, in which the OT is clearly detected (right). The OT absolute position, as measured relative to the USNO-A2 catalog (Monet et al. 1998), is R.A.(J2000.0) = $22^{\text{h}}07^{\text{m}}03.44^{\text{s}}$, decl.(J2000.0) = $-27^{\circ}48'51.9''$, with an rms of $0.2''$ in each axis. *HST* ACS data were reduced in the standard manner with the IRAF task *multidrizzle* (Fruchter & Hook 2002).

epochs. Image subtraction (Alard & Lupton 1998) of the first-epoch Gemini image from later epochs has revealed the presence of an OT (Ofek et al. 2006) spatially associated with the XRT position, within the galaxy 2dFGRS S173Z112 at $z = 0.0894$ (Colless et al. 2001; see Fig. 1). The position of the OT is R.A.(J2000.0) = $22^{\text{h}}07^{\text{m}}03.44^{\text{s}}$, decl.(J2000.0) = $-27^{\circ}48'51.9''$ (rms $0.2''$).

Given the possible low-redshift origin of this burst, we activated our *Hubble Space Telescope* (*HST*) target of opportunity program and observed GRB 060505 at two epochs, 14.36 and 32.8 days after the burst, using the Advanced Camera for Surveys (ACS). In each epoch we integrated for six orbits with the F475W (SDSS *g*) band and for three orbits with the F814W (Cousins *I*) band. The *HST* and Gemini images of the OT and host galaxy are presented in Figure 1.

The optical afterglow is not detected in the difference images of the two *HST* epochs down to a limiting AB magnitude of 27.3 and 27.1 in the F814W and F475W bands, respectively. It is also

not detected by subtraction of *Swift* UVOT images obtained at several epochs.

The log of optical imaging observations, along with the measurements and upper limits, is given in Table 1. All the limiting magnitudes were obtained by artificially adding point sources with decreasing magnitudes to the first-epoch images. To mimic the signal-to-noise ratio properties of the OT, we placed the artificial stars on top of a star-forming region in the host galaxy, which has a surface brightness similar to the one in the region where the OT was found. Then we subtracted the latest epoch from each simulated image and inspected the images for the artificial sources. Photometric calibration of the Gemini images was based on the *HST* imaging, which is presented, with details, in Table 2.

On 2006 May 13, we obtained a 2×30 minute spectrum of the position of the OT using the Gemini South telescope with the GMOS instrument. We used a $1''$ slit with the R400 grating blazed at 6000 \AA . The spectrum shows a feeble continuum emission and

TABLE 1
LOG OF OPTICAL OBSERVATIONS

Instrument	Date (UTC 2006)	Exp. Time (s)	Band	AB Mag (mag)	Flux (μ Jy)	
GMOS	May 06.377	5×180	<i>r</i>	21.93 ± 0.16	6.1 ± 1.0	
	May 06.393	5×240	<i>g</i>	22.43 ± 0.08	3.9 ± 0.3	
	May 12.316	5×180	<i>g</i>	>24.8	<0.43	
	May 12.330	5×180	<i>r</i>	>24.3	<0.69	
	May 14.353	5×180	<i>g</i>	>24.6	<0.52	
	May 14.367	5×180	<i>r</i>	>24.7	<0.48	
	May 14.380	5×180	<i>i</i>	≥ 23.3	≤ 1.7	
	May 26.318	10×300	<i>g</i>	... ^b	...	
	May 26.294	1×300	<i>r</i>	... ^b	...	
	UVOT ^a	May 05.981	834.7	<i>U</i>	>21.3	<10.7
May 10.512		1300.9	<i>U</i>	... ^b	...	
May 05.996		834.6	<i>V</i>	>20.4	<53	
May 21.818		11476.5	<i>V</i>	... ^b	...	
May 05.977		1666.3	UW1	>22.1	<5.8	
May 18.241		1735.6	UW1	... ^b	...	
May 05.999		2228.9	UM2	>23.7	<3.1	
May 10.505		3974.5	UM2	... ^b	...	
ACS		May 19.635	9×783	F814W	>27.3	<0.044
		May 19.636	18×783	F475W	>27.1	<0.053
	Jun 06.957	9×760	F814W	... ^b	...	
	Jun 07.160	18×760	F475W	... ^b	...	

^a *Swift* UVOT Vega-based zero points used are 17.29, 17.69, 18.38, and 17.88 mag for the UM2, UW1, *U*, and *V* bands, respectively. To convert Vega-based magnitudes to AB magnitudes, we added 1.65, 1.39, 0.99, and 0.00 mag to the UM2, UW1, *U*, and *V* bands, respectively.

^b Used as a reference image in the image subtraction process.

prominent emission lines at the redshift of the host galaxy, confirming that the bright knot at the OT position is indeed a star-forming region within the galaxy (see also Fynbo et al. 2006). In order to estimate the star formation rate within the host galaxy, on 2006 July 19 we obtained a flux-calibrated spectrum of the central part of the host galaxy using the Double Beam Spectrograph (DBSP) on the Palomar 200 inch (5 m) telescope. We used a 1'' slit with the R158 grating blazed at 7500 Å. The red-arm spectrum, shown in Figure 2, consists of two 15 minute exposures. An H α emission line is clearly detected in the spectrum, indicating ongoing star formation in this galaxy.

At about 19.2 days after the burst, we observed GRB 060505 using the ACIS-S detector on board *Chandra*. Using wvdetect,¹⁵ we identified a source consistent with the OT position. The source

was detected at the 3.5 σ confidence level in the 2–8 keV band. The XRT and *Chandra* X-ray measurements are listed in Table 3. The X-ray flux was calculated using WebPIMMS,¹⁶ assuming that the X-ray spectrum is described by a power law with a photon index of 2.0, and assuming a Galactic hydrogen column density of $N_{\text{H}} = 1.8 \times 10^{20} \text{ cm}^{-2}$ (Dickey & Lockman 1990). Figure 3 shows the X-ray and optical light curves of GRB 060505. The X-ray light curve is well fitted by a single power law with a slope of $\alpha_{\text{X}} = -1.33 \pm 0.17$ (*solid line*).

We have observed GRB 060505 with the Very Large Array,¹⁷ at a frequency of 8.46 GHz and with a 100 MHz bandwidth, at the following epochs: UTC 2006 May 17.53 and August 18.32,

¹⁶ Available at <http://cxc.harvard.edu/toolkit/pimms.jsp>.

¹⁷ The Very Large Array is operated by the National Radio Astronomy Observatory, a facility of the National Science Foundation operated under cooperative agreement by Associated Universities, Inc.

¹⁵ Part of the *Chandra* Interactive Analysis of Observations software.

TABLE 2
REFERENCE STARS

Name	R.A. (J2000.0)	Decl. (J2000.0)	<i>g</i> (AB mag ^a)	<i>r</i> (AB mag ^a)	<i>i</i> (AB mag ^a)
S1 ^b	22 07 02.95	-27 48 44.4	19.70 ± 0.02	19.35 ± 0.02	19.26 ± 0.02
S2 ^c	22 07 03.15	-27 48 46.5	20.95 ± 0.03	19.61 ± 0.06	19.16 ± 0.02

NOTE.—Units of right ascension are hours, minutes, and seconds, and units of declination are degrees, arcminutes, and arcseconds.

^a The magnitudes were calculated by fitting the synthetic photometry magnitudes of stellar spectral templates (Pickles 1998) to the observed ACS F475W- and F814W-band magnitudes and then calculating the synthetic magnitudes in the *g*, *r*, and *i* bands, using the best-fit spectral template. The ACS magnitudes were measured in a 4 pixel radius aperture and were extrapolated to an infinite aperture (Sirianni et al. 2005).

^b The best-fit spectral template for this object is of an F8 V star. The ACS F475W magnitude is 19.69 ± 0.02 , and the ACS F814W magnitude is 19.24 ± 0.02 .

^c The best-fit spectral template for this object is of a K3 I star. The ACS F475W magnitude is 20.90 ± 0.03 , and the ACS F814W magnitude is 19.04 ± 0.02 .

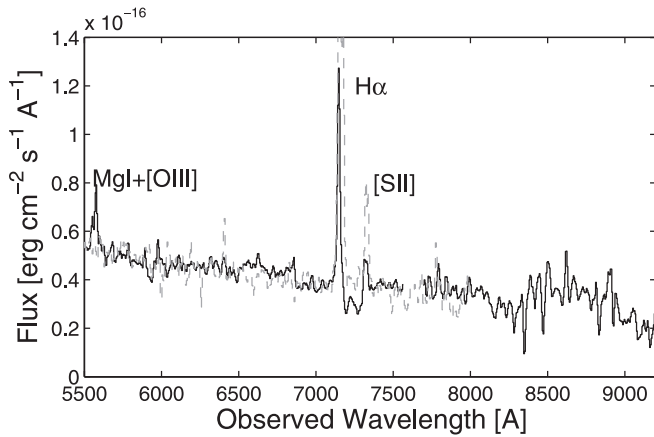


FIG. 2.—Spectrum of the host galaxy of GRB 060505 obtained by the DBSP mounted on the Palomar observatory 200 inch telescope (solid black line). The spectrum continuum shape and emission lines, as well as the galaxy morphology (Fig. 1), are typical for an Sc galaxy. However, we note that we do not identify the absorption features redward of the $H\alpha$ line. A scaled spectrum template of an Sc galaxy (Kinney et al. 1996) redshifted to match the host galaxy is shown with the gray dashed line. The gap around 7600 Å is due to removal of telluric absorption.

20.35, 21.32, 22.31, and 23.37. The reduction was done following standard practice in the Astronomical Image Processing System (AIPS) software package. At the first epoch, 12.3 days after the burst, no radio source was visible at the OT position to a 3σ limit of 165 μJy . Summing the last five epochs, with a mean epoch of 107.8 days after the burst, reveals no radio source to a 3σ limit of 46 μJy at the OT position.

3. RESULTS

At $z = 0.0894$, the luminosity distance¹⁸ to GRB 060505 is 404 Mpc (distance modulus 38.03 mag; angular diameter distance 341 Mpc). The relatively low redshift of GRB 060505 makes it an extraordinary event, both for constraining the presence of a supernova and the ejecta from the explosion and for studying the GRB environment. We discuss these issues below.

3.1. Environment and Progenitor Age

As seen in Figure 1, GRB 060505 is spatially associated with a bright, spectroscopically confirmed star-forming region found at a projected distance of 7.1 kpc ($4.3''$) from its host galaxy center.

¹⁸ We assume *WMAP* and SDSS cosmological parameters: $H_0 = 70.9 \text{ km s}^{-1} \text{ Mpc}^{-1}$, $\Omega_m = 0.266$, and $\Omega_\Lambda = 1 - \Omega_m$ (Spergel et al. 2007).

The AB magnitudes of this star-forming knot are 23.9 and 23.7 in the F475W and F814W bands, respectively.

Our observations (Figs. 1 and 2) show that 2dFGRS S173Z112 is a face-on Sc-type galaxy. Using the flux of the $H\alpha$ emission line, along with the relation from Kennicutt (1998), we estimate that the star formation rate in this galaxy is about $2 M_\odot \text{ yr}^{-1}$. We obtained this value by extrapolating the $H\alpha$ emission, observed within the slit, over the entire area of the galaxy, weighted by the g -band surface brightness. We note that the total AB magnitudes of the galaxy are 18.3 and 17.7 in the F475W and F814W bands, respectively. This is equivalent to absolute magnitudes of -19.4 and -20.4 in the F475W and F814W bands, respectively (K -corrected; Oke & Sandage 1968). Therefore, the specific star formation in this galaxy is $\sim 3 M_\odot \text{ yr}^{-1} L_*^{-1}$.

The association of GRB 060505 with a bright star-forming region can be used to set a limit on the delay time from progenitor birth to explosion. This limit may be especially interesting if GRB 060505 is a consequence of a compact-binary merger rather than being due to a massive star's core collapse. First, the presence of an H II region at the explosion site of GRB 060505 suggests a delay time below $\sim 10 \text{ Myr}$ (e.g., Mayya 1995). Second, a limit on the delay time that is applicable for the compact-star merger scenario can be derived from the size of the star-forming region combined with the speed of the progenitor. The diameter of $d \sim 400 \text{ pc}$ of the H II region at the position of the OT suggests that the delay time, τ , from birth to explosion of GRB 060505 is

$$\tau \lesssim 11 \times 10^6 \frac{d}{400 \text{ pc}} \left(\frac{v}{35 \text{ km s}^{-1}} \right)^{-1} \text{ yr}, \quad (1)$$

where v is the (kick) velocity of the progenitor. The 35 km s^{-1} kick velocity we adopted is half (in order to account for the binary center of mass speed) of the value of the lowest transverse velocity of a pulsar in the sample of Hansen & Phinney (1997).

3.2. Supernova Limits

The absence of detectable optical emission from the OT at ≥ 2 days after the burst (see Table 1) suggests that GRB 060505 was not associated with a bright supernova. If we assume negligible extinction,¹⁹ our deep *HST* observations imply a limit on the g - and i -band absolute magnitude of a supernova, 2 weeks after the burst, of $\geq -11 \text{ mag}$. Extinction within the host galaxy may weaken

¹⁹ The Galactic extinction toward GRB 060505 is $E_{B-V} = 0.02$ (Schlegel et al. 1998).

TABLE 3
LOG OF X-RAY OBSERVATIONS

Date ^a	Telescope	Exp. (ks)	Band ^b (keV)	Count Rate (counts s ⁻¹)	Γ^c	Flux ^d (erg s ⁻¹ cm ⁻²)	Flux ^e (nJy)
05.973.....	<i>Swift</i>	8.0	0.2–10	$(1.1 \pm 0.1) \times 10^{-2}$	2.0	$(4.6 \pm 0.4) \times 10^{-13}$	49.2
					2.5	$(4.2 \pm 0.4) \times 10^{-13}$	45.5
10.031.....	<i>Swift</i>	11.7	0.2–10	$(8.6 \pm 4.0) \times 10^{-4}$	2.0	$(3.6 \pm 1.7) \times 10^{-14}$	3.84
					2.5	$(3.3 \pm 1.5) \times 10^{-14}$	3.55
24.334.....	<i>Chandra</i>	24.71	2.0–8	$(1.2^{+1.6}_{-0.9}) \times 10^{-4}$	2.0	$(5.4^{+6.9}_{-3.9}) \times 10^{-15}$	0.571
					2.5	$(9.4^{+12}_{-6.7}) \times 10^{-15}$	0.997

NOTE.—*Swift* XRT X-ray counts are from Conciatore (2006).

^a UTC 2006 May, time of beginning of observation.

^b Band for the X-ray counts.

^c Photon index assumed in the conversion from counts to flux.

^d Unabsorbed flux in the 0.2–10 keV band. We assume a Galactic neutral hydrogen column density of $N_{\text{H}} = 1.8 \times 10^{20} \text{ cm}^{-2}$ (Dickey & Lockman 1990).

^e Specific flux at 1 keV.

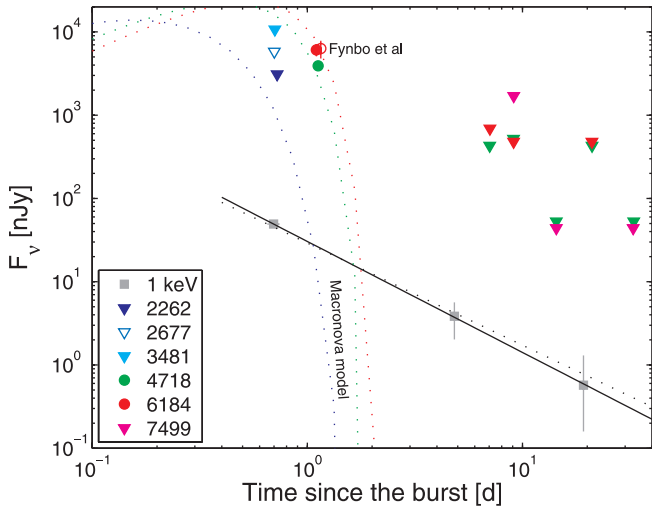


FIG. 3.—X-ray (gray squares) and optical (colored circles and triangles) light curves of GRB 060505 (see Tables 1 and 3). The circles represent the optical measurements, while the triangles mark upper limits. The wavelength of each measurement is color-coded and shown in the legend (in units of angstroms or keV), where the numbers 2262, 2677, 3481, 4718, 6184, and 7499 correspond to the UM2, UW1, U , g , r , and i bands, respectively. The red, green, and blue dotted lines show a macronova model with an ejecta mass of $3 \times 10^{-2} M_{\odot}$ and ejecta velocity of 0.6 times the speed of light, in the UM2 (2262 Å), g (4718 Å), and r (6184 Å) bands, respectively (see Kulkarni 2005 for details). In the conversion of the X-ray counts to flux, we assumed that the X-ray spectrum is described by a power law with a photon index of 2.0. The solid black line shows the best-fit power law to the X-ray data, with an index of $\alpha_X = -1.33 \pm 0.17$ ($\chi^2/\text{dof} = 0.005/1$). Assuming a power law with a photon index of 2.5 gives $\alpha_X = -1.22 \pm 0.16$ ($\chi^2/\text{dof} = 0.3/1$; dotted black line).

our results. However, the Balmer lines ratio of the star formation region at the position of the OT is suggestive of no reddening (Fynbo et al. 2006). We note that the color of the afterglow ($f_{\nu} \propto \nu^{-1.7 \pm 0.7}$) is somewhat redder than that expected for GRB afterglow. Therefore, it may suggest some extinction. We put a conservative upper limit on the extinction by using the observed color of the OT at 1 day after the burst and by assuming that the intrinsic optical spectrum cannot be steeper than a Rayleigh-Jeans spectrum ($f_{\nu} \propto \nu^2$). We find that $E_{B-V} < 1.04$ (assuming $A_V/E_{B-V} = 3.08$; Cardelli et al. 1989).

If we assume this “maximal extinction,” the i -band absolute AB magnitude of a supernova lurking in the OT position is fainter than -12.6 . This limit includes a K -correction (Humason et al. 1956; $m_{\text{int}} = m_{\text{obs}} - K$) of 0.05 mag in the i band, if we assume an SN 1998bw–like spectrum. Our limit improves on the result of Fynbo et al. (2006) by 3 mag (at about 2 weeks after the burst) and rules out even the faint class of supernova that they discuss.

Furthermore, using our *HST* limit on day 14, along with equation (44) in Kulkarni (2005), we can place an approximate upper limit on the mass of the radioactive ^{56}Ni produced in this explosion: $M_{^{56}\text{Ni}} \lesssim 2 \times 10^{-4} M_{\odot}$, assuming no extinction, and $M_{^{56}\text{Ni}} \lesssim 10^{-3} M_{\odot}$, assuming maximal extinction. We note that the faintest core-collapse supernovae known to date ejected about $(2-8) \times 10^{-3} M_{\odot}$ of ^{56}Ni (e.g., Pastorello et al. 2004), but there may be a bias against finding such low-luminosity SNe.

3.3. The Light Curve and Spectral Energy Distribution

As shown in Figure 3, the light curve of this GRB is not well constrained. At later times, between days 1 and 14, the power-law index is steeper than about -1.9 . The X-ray light curve, on the other hand, is consistent with a single power-law decay rate of $\alpha_X = -1.33 \pm 0.17$.

Although the optical-to-X-ray spectral power-law index $\beta_{\text{ox}} = -0.80 \pm 0.03$ (defined by $f_{\nu} \propto \nu^{\beta_{\text{ox}}}$) that we measured at 1.1 days after the burst is typical for GRB afterglows, the visible-light color of the afterglow ($f_{\nu} \propto \nu^{-1.7 \pm 0.7}$) is marginally redder than that expected at 1 day after the burst (e.g., Šimon et al. 2001; Lipkin et al. 2004). Possible explanations are either that the OT is reddened or that some of the optical radiation is contributed by some additional mechanism (i.e., not by the afterglow). An interesting possibility is that the early optical emission is powered, in addition to the afterglow light, by the decay of free neutron ejecta. Such a scenario was suggested in the context of neutron star (NS) mergers by Li & Paczyński (1998) and investigated by Kulkarni (2005; i.e., macronova). In Figure 3 we show, for example, a macronova model that is roughly consistent with the optical data. The dotted red, green, and blue lines correspond to a macronova model with $3 \times 10^{-2} M_{\odot}$ free neutron ejecta and a velocity of 0.6 times the speed of light. An inspection of the models presented by Kulkarni (2005) suggests that the radioactive decay of the free neutron ejecta may roughly explain the behavior of the optical light curve. However, our observations are too sparse for a critical examination of this model.

4. DISCUSSION

GRBs are traditionally classified according to their durations into short and long events (Kouveliotou et al. 1993). GRB 060505 has some unusual characteristics that make it difficult to place within this scheme. Fynbo et al. (2006) suggested that GRB 060505 may belong to a newly emerging group of long-duration GRBs without a supernova. We note that the existence of a third group of GRBs was already suggested in the past (e.g., Mukherjee et al. 1998; Horváth 2002), based on the analysis of the GRB duration distribution. Recently, a third group was also discussed by Gal-Yam et al. (2006), Fynbo et al. (2006), and Della Valle et al. (2006), who presented observations of GRB 060614: a long-duration GRB ($T_{90} \approx 102$ s; Barthelmy et al. 2006) spatially associated with a $z = 0.125$ galaxy, but with no apparent supernova. However, a simpler explanation for this particular case is that GRB 060505 was a short-duration GRB. We note that “short” is used here in the sense that the GRB physical mechanism is similar to that of short GRBs. We discuss the various possibilities for the nature of GRB 060505 below.

The absence of a supernova, the low isotropic equivalent gamma-ray energy, $E_{\gamma, \text{iso}} = (1.2 \pm 0.2) \times 10^{49}$ erg, and the low redshift of GRB 060505 are characteristic of other short-duration GRBs (see, however, Berger et al. 2007). On the other hand, the duration of GRB 060505 is above the canonical 2 s cut that separates short and long GRBs. However, the duration distributions of short and long GRBs overlap (e.g., Horváth 2002; Donaghy et al. 2006). For example, if we adopt the Horváth (2002) decomposition (based on BATSE observations), the probability of a short burst to have a T_{90} duration larger than 4 s is about 12%. Moreover, 64% of the GRBs with ~ 4 s durations belong to the “short”-duration group. Although the Horváth (2002) decomposition is not necessarily the correct one, it is preferred over using a sharp cutoff at 2 s.

If indeed GRB 060505 is a genuine short-duration GRB, then our limit on the delay time implies that any scenario for short-duration GRBs should be able to produce events with delay times shorter than about 10 Myr. In the context of the NS merger scenario, we note that Belczynski et al. (2006) estimated that the probability function for the time delay from binary birth to explosion has a narrow maximum around 20 Myr with approximately 10 Myr width, followed by a flat probability extending to delay

times on the order of the Hubble time. Furthermore, NS–black hole (BH) mergers may have somewhat shorter delay times than NS–NS mergers. Therefore, if indeed GRB 060505 was a short-duration GRB, our observations are consistent with a NS–NS or NS–BH merger model for short GRBs.

Next we address the possibility that GRB 060505 is a long-duration GRB. The redshift and the isotropic equivalent gamma-ray energy of GRB 060505 are atypically low for a “classical” long GRB. While several anomalous low-energy, local universe, long GRBs have been detected (e.g., GRB 060218; Campana et al. 2006), GRB 060505 and GRB 060614 (Gal-Yam et al. 2006) are not associated with a supernova.

Following Fruchter et al. (2006), we compared the environment of GRB 060505 to that of other long GRBs. Fruchter et al. (2006) studied a sample of long GRBs with identified host galaxies. They sorted all the pixels in each host galaxy image by brightness and computed the fraction of the total light of the host contained in pixels that were fainter than or equal in brightness to the pixel in which the OT was located. Next they presented a histogram of this fraction of light, and they found that long GRBs prefer to reside in the brightest pixels of a galaxy. We applied the Fruchter et al. (2006) analysis to an F475W-band image of GRB 060505. Using exactly the same SExtractor (Bertin & Arnouts 1996) detection criteria used by these authors, we find that the brightness at the spatial position of the OT is within the dimmest 1%–45% (depending on the exact location of the OT, which is known to about 60 mas) of the galaxy light. Comparing this to the long-duration GRB population investigated by Fruchter et al. (2006), we find that fewer than 10% of the Fruchter et al. (2006) long-duration GRBs occurred in regions similar to (or fainter than) that of GRB 060505. We note that our analysis may be biased by two facts. First, our observations were made at rest-frame wavelengths of about 4400 Å, while the Fruchter et al. (2006) analysis was performed at a median rest-frame wavelength of about 3700 Å. However, as shown by Fruchter et al. (2006), their analysis is not sensitive to the redshift of the galaxies in their sample. Second, the redshift of GRB 060505 is smaller (by a factor of ~ 9) than the typical redshift of the GRBs in the Fruchter et al. (2006) sample. Placing our galaxy at the typical redshift of the Fruchter et al. sample will bring most of the galaxy light below the noise level. Hence, the fraction of observable galaxy light that is dimmer than the brightness at the OT position decreases, making GRB 060505 less consistent with the long-duration GRB population. We note that a possible interpretation of the Fruchter et al. analysis is that long GRBs are associated with low-metallicity environments. Therefore, long GRBs in massive spiral galaxies are expected to occur at the outskirts of the galaxy, where the metallicity is on average lower. In this case the fact that GRB 060505 occurred in the outer region of its host galaxy may support the notion that it is a long GRB. Therefore, it will be constructive to measure the metallicity of the GRB 060505 host galaxy and the immediate environment of the GRB and to compare it with the metallicity of other long GRB hosts.

Fynbo et al. (2006) suggested that both GRB 060505 and GRB 060614 may constitute a new class of GRBs that are associated with faint supernovae (e.g., Fryer et al. 2006). If a class of long

GRBs with faint supernovae (or none) exists, a clue regarding the nature of the progenitor can be derived from the rate of such events, which we derive below. To estimate the rate, we took into account the BAT field of view (1.4 sr) and operation time (1.67 yr) and assumed that at least two such bursts were observed by the *Swift* BAT. Next we summed the volume of the two GRBs and multiplied it by 2. We introduced the factor of 2 in order to account for the fact that we can detect bursts at larger distances. It has been shown (Schmidt 1968) that the expectancy value for the ratio of the volume enclosed within the distance to an event to the maximal volume in which such an event is detectable (i.e., V/V_{max}) is 1/2; hence the factor of 2. We find that the local rate of such GRBs is $\geq 1.5 \text{ yr}^{-1} \text{ Gpc}^{-3}$, at the 95% confidence level (Gehrels 1986). This lower limit is approximately 3 times larger than the observed rate of classical long GRBs (without beaming correction; e.g., Schmidt 2000; Guetta et al. 2005). However, this limit is below the inferred rate of low-luminosity long GRBs such as GRB 980425 and GRB 060218 (e.g., Soderberg et al. 2006).

Finally, we discuss the possibility that GRB 060505 is a background event unrelated to the galaxy 2dFGRS S173Z112. Schaefer & Xiao (2006) claimed that the association of GRB 060505 with the galaxy 2dFGRS S173Z112 is due to a chance coincidence. Estimating the probability for a chance coincidence is susceptible to the pitfalls of a posteriori statistics. Moreover, it is not clear how to incorporate additional information, such as the fact that GRB 060505 is associated with a star-forming region. Bearing this in mind, we note that in their calculation Schaefer & Xiao (2006) used an inappropriate luminosity (of $0.03L_*$) for the host galaxy of GRB 060505. Repeating their calculation using the correct value ($0.67L_*$), and using the galaxy luminosity function given by Blanton et al. (2003), we find that the probability for a chance coincidence per trial is 6 times lower than the probability of 0.8% claimed by Schaefer & Xiao (2006). While a chance projection cannot be definitely ruled out for this burst, its association with 2dFGRS S173Z112 is no less certain than those of prototypical short GRBs (e.g., GRB 050709 and GRB 050724) with their host galaxies.

To summarize, our observations show that GRB 060505 is not associated with any supernova brighter than an absolute *i*-band magnitude of -11 (assuming no extinction). Furthermore, we can constrain the mass of radioactive ^{56}Ni ejecta to be less than $2 \times 10^{-4} M_{\odot}$, and we find that the delay time from birth to explosion of this GRB progenitor is probably smaller than ~ 10 Myr. The simplest interpretation of GRB 060505 is that it is the nearest observed short-duration GRB to date. Another possibility is that GRB 060505 belongs to a new class of supernova-lacking GRBs that have long durations. However, this would require the rate of such events to be at least a factor of 3 larger than that of “classical” long GRBs.

E. O. O. thanks Orly Gnat for valuable discussions and the anonymous referee for useful comments. This work is supported in part by grants from NSF and NASA.

REFERENCES

- Alard, C., & Lupton, R. H. 1998, *ApJ*, 503, 325
 Barthelmy, S., et al. 2006, *GCN Circ.* 5256, <http://gcn.gsfc.nasa.gov/gcn/gcn3/5256.gen3>
 Belczynski, K., Perna, R., Bulik, T., Kalogera, V., Ivanova, N., & Lamb, D. Q. 2006, *ApJ*, 648, 1110
 Berger, E., et al. 2005, *Nature*, 438, 988
 ———. 2007, *ApJ*, in press (astro-ph/0611128)
 Bertin, E., & Arnouts, S. 1996, *A&AS*, 117, 393
 Blanton, M. R., et al. 2003, *ApJ*, 592, 819
 Bloom, J. S., et al. 2006, *ApJ*, 638, 354
 Brown, P. J., & Palmer, D. 2006, *GCN Circ.* 5082, <http://gcn.gsfc.nasa.gov/gcn/gcn3/5082.gen3>
 Campana, S., et al. 2006, *Nature*, 442, 1008
 Cardelli, J. A., Clayton, G. C., & Mathis, J. S. 1989, *ApJ*, 345, 245

- Colless, M., et al. 2001, MNRAS, 328, 1039
- Conciatore, M. L. 2006, GCN Circ. 5115, <http://gcn.gsfc.nasa.gov/gcn/gcn3/5115.gcn3>
- Conciatore, M. L., Capalbi, M., Vetere, L., Palmer, D., & Burrows, D. 2006, GCN Circ. 5078, <http://gcn.gsfc.nasa.gov/gcn/gcn3/5078.gcn3>
- Della Valle, M., et al. 2006, Nature, 444, 1050
- Dickey, J. M., & Lockman, F. J. 1990, ARA&A, 28, 215
- Donaghy, T. Q., et al. 2006, ApJ, submitted (astro-ph/0605570)
- Fox, D. B., et al. 2005, Nature, 437, 845
- Fruchter, A. S., & Hook, R. N. 2002, PASP, 114, 144
- Fruchter, A. S., et al. 2006, Nature, 441, 463
- Fryer, C. L., Young, P. A., & Hungerford, A. L. 2006, ApJ, 650, 1028
- Fynbo, J. P. U., et al. 2006, Nature, 444, 1047
- Gal-Yam, A., et al. 2006, Nature, 444, 1053
- Gehrels, N. 1986, ApJ, 303, 336
- Gehrels, N., et al. 2005, Nature, 437, 851
- Guetta, D., Piran, T., & Waxman, E. 2005, ApJ, 619, 412
- Hansen, B. M. S., & Phinney, E. S. 1997, MNRAS, 291, 569
- Hjorth, J., et al. 2005, Nature, 437, 859
- Horváth, I. 2002, A&A, 392, 791
- Hullinger, D., et al. 2006, GCN Circ. 5142, <http://gcn.gsfc.nasa.gov/gcn/gcn3/5142.gcn3>
- Humason, M. L., Mayall, N. U., & Sandage, A. R. 1956, AJ, 61, 97
- Kennicutt, R. C., Jr. 1998, ApJ, 498, 541
- Kinney, A. L., Calzetti, D., Bohlin, R. C., McQuade, K., Storchi-Bergmann, T., & Schmitt, H. R. 1996, ApJ, 467, 38
- Kouveliotou, C., Meegan, C. A., Fishman, G. J., Bhat, N. P., Briggs, M. S., Koshut, T. M., Paciesas, W. S., & Pendleton, G. N. 1993, ApJ, 413, L101
- Kulkarni, S. R. 2005, preprint (astro-ph/0510256)
- Li, L.-X., & Paczyński, B. 1998, ApJ, 507, L59
- Lipkin, Y. M., et al. 2004, ApJ, 606, 381
- Mayya, Y. D. 1995, AJ, 109, 2503
- Monet, D. B. A., et al. 1998, The USNO-A2.0 Catalog (Washington, DC: USNO)
- Mukherjee, S., Feigelson, E. D., Babu, G. J., Murtagh, F., Fraley, C., & Raftery, A. 1998, ApJ, 508, 314
- Nakar, E. 2007, in the *Bethe Centennial Volume of Physics Reports*, ed. G. E. Brown, V. Kalogera, & E. P. J. van den Heuvel, in press (astro-ph/0701748)
- Ofek, E. O., Cenko, S. B., Gal-Yam, A., Peterson, B., Schmidt, B. P., Fox, D. B., & Price, P. A. 2006, GCN Circ. 5123, <http://gcn.gsfc.nasa.gov/gcn/gcn3/5123.gcn3>
- Oke, J. B., & Sandage, A. 1968, ApJ, 154, 21
- Palmer, D., Cummings, J., Stamatikos, M., Markwardt, C., & Sakamoto, T. 2006, GCN Circ. 5076, <http://gcn.gsfc.nasa.gov/gcn/gcn3/5076.gcn3>
- Pastorello, A., et al. 2004, MNRAS, 347, 74
- Pickles, A. J. 1998, PASP, 110, 863
- Schaefer, B. E., & Xiao, L. 2006, ApJL, submitted (astro-ph/0608441)
- Schlegel, D. J., Finkbeiner, D. P., & Davis, M. 1998, ApJ, 500, 525
- Schmidt, M. 1968, ApJ, 151, 393
- . 2000, in *AIP Conf. Proc. 526, Gamma-Ray Bursts*, 5th Huntsville Symposium, ed. R. M. Kippen, R. S. Mallozzi, & G. J. Fishman (New York: AIP), 58
- Šimon, V., Hudec, R., Pizzichini, G., & Masetti, N. 2001, A&A, 377, 450
- Sirianni, M., et al. 2005, PASP, 117, 1049
- Soderberg, A. M., et al. 2006, Nature, 442, 1014
- Spergel, D. N., et al. 2007, ApJS, in press (astro-ph/0603449)
- Thöne, C. C., Fynbo, J. P. U., Sollerman, J., Jensen, B. L., Hjorth, J., Jakobsson, P., & Klose, S. 2006, GCN Circ. 5161, <http://gcn.gsfc.nasa.gov/gcn/gcn3/5161.gcn3>